Title

Functional characterization of alternatively spliced GSN in head and neck squamous cell carcinoma

Authors

Kelley, Dylan Z
Flam, Emily L
Guo, Theresa
et al.

Publication Date

2018-12-01

DOI

10.1016/j.trsl.2018.07.007

Peer reviewed

HHS Public Access

Author manuscript

Transl Res. Author manuscript; available in PMC 2019 December 01.

Published in final edited form as:

Transl Res. 2018 December ; 202: 109–119. doi:10.1016/j.trsl.2018.07.007.

Functional characterization of alternatively spliced *GSN* in head and neck squamous cell carcinoma.

Kelley DZ[a], **Flam EL**[a], **Guo T**[a], **Danilova LV**[b,c], **Zamuner F**[a], **Bohrson C**[b], **Considine M**[b], **Windsor EJ**[d], **Bishop JA**[e], **Zhang C**[a], **Koch WM**[a], **Sidransky D**[a], **Westra WH**[e], **Chung CH**[b], **Califano JA**[f,g], **Wheelan S**[b], **Favorov AV**[b,c], **Florea L**[h], **Fertig EJ**[b,i], and **Gaykalova DA**[a]

[a]Department of Otolaryngology-Head and Neck Surgery, Johns Hopkins University School of Medicine, Baltimore, MD, 21231, USA

[b]Department of Oncology, The Sidney Kimmel Comprehensive Cancer Center, Johns Hopkins University School of Medicine, 1550 Orleans Street, Baltimore, MD, 21231, USA

[c]Laboratory of Systems Biology and Computational Genetics, Vavilov Institute of General Genetics, Russian Academy of Sciences, Moscow, Russia

[d]Department of Biotechnology, Maryland Holistics LLC, Ellicott City, MD, 21043, USA

[e]Department of Pathology, Johns Hopkins Medical Institutions, Baltimore, MD, 21205, USA

[f]Head and Neck Cancer Center, Moores Cancer Center, University of California, San Diego, 3855 Health Sciences Dr., MC 0803, La Jolla, CA, 92093, USA

[g]Division of Otolaryngology-Head and Neck Surgery, Department of Surgery, 3855 Health Sciences Dr., MC 0803, La Jolla, CA, 92093, USA

[h]McKusick-Nathans Institute of Genetic Medicine, Center for Computational Biology, Johns Hopkins University School of Medicine, Baltimore, MD, 21205, USA

[i]Department of Otolaryngology – Head and Neck Surgery (OHNS), University of California, San Francisco, CA, 94143, USA

Abstract

We have recently performed the characterization of alternative splicing events (ASEs) in head and neck squamous cell carcinoma (HNSCC), which allows dysregulation of protein expression common for cancer cells. Such analysis demonstrated a high ASE prevalence amongst tumor samples, including tumor-specific alternative splicing in the *GSN* gene. *In vitro* studies confirmed that overall expression of either *ASE-GSN* or wild-type *GSN* (*WT-GSN*) isoform inversely correlated with cell proliferation, whereas the high ratio of *ASE-GSN* to *WT-GSN* correlated with increased cellular invasion. Additionally, a change in expression of either isoform caused compensatory changes in expression of the other isoform. Our results suggest that the overall

Corresponding Author: Daria A. Gaykalova – 1550 Orleans St, Rm 5M05C, Cancer Research Building II, Baltimore, MD, 21231, USA - Phone: 410.614.2745 - Fax: 410.614.1411 - dgaykal@jhmi.edu.

expression and the balance between *GSN* isoforms are mediating factors in proliferation, while increased overall expression of *ASE-GSN* is specific to cancer tissues. As a result, we propose *ASE-GSN* can serve not only as a biomarker of disease and disease progression, but also as a neoantigen for HNSCC treatment, for which only a limited number of disease-specific targeted therapies currently exist.

BACKGROUND

Head and neck squamous cell carcinoma (HNSCC) is a disease with an insufficient number of targeted therapeutics and biomarkers currently used in clinical practice. The detection of alternative splicing events (ASE) allows for the discovery of both biomarkers and therapeutic targets.

Keywords

Head and Neck Squamous Cell Carcinoma (HNSCC); Alternative Splicing Event (ASE); Gelsolin (*GSN*)

INTRODUCTION:

Alternative splicing events allow for the formation of variant transcripts and increased protein functional diversity. (1, 2) Previous studies have shown that some cancers express increased transcript variants due to alternative splicing events. (3, 4) We hypothesized that alternative splicing might be one of the mechanisms by which dysregulation occurs in cancer, which may result in the oncogenic transformation of cells (altered cell proliferation, apoptosis, invasion, and migration). To explore this hypothesis, our group has recently performed a whole-genome evaluation of ASEs in Head and Neck Squamous Cell Carcinoma (HNSCC), a disease that is characterized by abundant gene expression dysregulation. (5) Limited advancement has been made toward predicting HNSCC tumor recurrence, aggression, and improving the identification of targeted and disease-specific treatment. (6, 7)

HNSCC is treated by surgical resection, radiation therapy, chemotherapy (Cetuximab), or molecular targeted therapy (Pembrolizumab/Nivolumab). Cetuximab is a monoclonal antibody against EGFR, (8) Pembrolizumab, (9) and Nivolumab (10) are monoclonal antibodies targeting PD1, (7, 11) the only targeted therapeutics approved for all Head and Neck patients. These therapies offer greater curative power with fewer adverse effects than traditional regimens, but current targeted therapeutics still involve serious adverse reactions in almost half of patients receiving treatment. (10) Further investigation is needed to identify therapeutic options with fewer adverse effects on patient health. ASEs have the potential to serve not only as cancer-specific biomarkers, but also as neoantigens for novel targeted therapeutics.

In our recent paper, RNA-Seq, a next-generation sequencing technology, was used to define the whole-genome distribution of ASE in HNSCC. (2) Using Outlier Gene Set Analysis (OGSA), (12, 13) we detected and validated 109 significant ASEs. The *GSN* (gelsolin) gene,

which codes for an actin-binding protein that plays a role in PI3K/AKT/mTOR pathway, was detected as one of the most abundant ASEs in this cohort (present in 34% of HNSCC samples). (2, 14) Furthermore, ASE in *GSN* was detected in the pan-cancer analysis of RNA-Seq from TCGA as leading alternative splicing in HNSCC, along with ASE detected in *TNC* and *CAB39L*. (15) ASE in *GSN* was also detected in breast invasive carcinoma and kidney chromophobe. (15) Additionally, downregulation of *GSN* has been shown to downregulate apoptosis, a hallmark of cancer cells. (16–19) From these data, we hypothesized that alternative splicing in GSN causes malignant cell transformation, but no functional analysis for the alternatively-spliced GSN was ever performed before our work. Herein, we demonstrate that different *GSN* transcripts (WT and ASE) affect cellular carcinogenic characteristics. Furthermore, the abundance of *ASE-GSN* in cancer cases indicates that utilization of *ASE-GSN* as neoantigen has a direct clinical application and significance not only for head and neck cancers, but also for other tumor types.

MATERIALS AND METHODS:

Human subject research

All human samples were obtained from previously published collections in accordance with Institutional Review Board Guidelines. (2) No new human samples were collected for this study.

RNA-Seq data and processing

Primary RNA-Seq data from Johns Hopkins patient samples were retrieved, normalized, and analyzed as described in our previous publications. (2) ASE-junction expression was detected as RPM (reads per million), and WT-junction expression was detected as RSEM (RNA-Seq by expectation-maximization) using the available RNA-Seq data. (2, 14)

Cell lines and cell culture

Human HNSCC cell lines UM-SCC-22B and SCC61 were provided by Dr. Thomas Carey from the University of Michigan and Ralph Weichselbaum from the University of Chicago, respectively. These cells were used for functional evaluation of the ASE-GSN, due to their increased cellular mobility, needed for the completion of cell invasion assays. Each cell line was authenticated using a Short Tandem Repeat (STR) Identifier kit (Applied Biosystems). UM-SCC-22B cells were cultured in DMEM (Invitrogen) High Glucose supplemented with 10% Fetal Bovine Serum (Gemini) mixed with X1 Penicillin and Streptomycin (Corning). SCC61 cell line was cultured in DMEM/F12 (Invitrogen) supplemented with 10% Fetal Bovine Serum mixed with Penicillin and Streptomycin. All cultured cell growth occurred in a 5 % CO_2 incubator at 37° C. Cell lines enumerated in **Supplemental Table 1** were analyzed for *ASE-GSN* and *WT-GSN* expression using available RNA from our previous publication. (20)

Transient transfections

Ectopic expression—The ectopic expression of human *WT-GSN* and *ASE-GSN* was performed using commercial (*WT-GSN*, RC214871) and custom (*ASE-GSN*) plasmids with mammalian cDNA expressing pCMV6-Entry Vector (OriGene). Since ASE-GSN has an

early stop codon in frame encoded in the intronic sequence (**Supplemental Fig 1**), the ASE-GSN plasmid contains the GSN sequence before this stop codon. Plasmid transfections were performed in parallel with empty pCMV6-Entry Vectors (21) in Opti-MEM (Invitrogen) culture medium using X-tremeGENE 9 DNA Transfection Reagent (Roche) per manufacturer instructions. The transfection efficiency and the level of the ectopic gene and protein expression were monitored by qRT-PCR and Western Blotting, respectively.

RNA interference experiments—ON-TARGETplus Human GSN pool (L-007775–00-0005) of four siRNA targeting sequences CUGUUGAGGUAUUGCCUAA, GCUAAGCGGUACAUCGAGA, GCACUGAACUCCAACGAUG, and GAACGGAAAUCUGCAGUAU (Dharmacon) was used to downregulate the expression of *WT-GSN*. It was challenging to design siRNA for efficient downregulation of *ASE-GSN*. Out of four custom designed ON-TARGETplus Human *ASE-GSN* siRNA, two of these downregulated ASE-GSN expression. These siRNA were labeled siRNA1 (targeting sequence GACCAGAUCUCCAGGCACAUU) and siRNA2 (targeting sequence GGCAGGGGAUGGUGAAUGAUU) (Dharmacon). Transfection of pooled or single siRNAs was performed in Opti-MEM (Invitrogen) using RNAiMAX Lipofectamine Reagent (Invitrogen) in parallel with ON-TARGETplus Pool (D-001810–10) controls. The transfection efficiency and the level of the endogenous gene and protein expression were monitored by qRT-PCR and Western Blotting, respectively.

Cell proliferation

The cellular growth-monitoring experiments were performed in 96-well plates with five independent wells per experiment. The cells were incubated for one hour in 100 μL of 1:10 diluted Alamar Blue (Bio-Rad) (22) and Opti-MEM Media (Invitrogen). Fluorescence was observed by exciting at 530 nm and detecting emission at 590 nm on Spectramax M2.

Invasion Assay

Matrigel invasion assays (23) were performed in 6.5mm Transwell® with 8.0μm Pore Polycarbonate Membrane Inserts (Corning) covered by 100 μL of diluted Matrigel (Corning) in serum-free DMEM High Glucose medium (Invitrogen) set up in 37° C overnight. Before plating cells on the top of solidified Matrigel, cells were washed three times with cold, serum-free DMEM High Glucose medium (Invitrogen). Cells were chemo-attracted to invade through the Matrigel and the membrane toward DMEM High Glucose medium (Invitrogen) supplemented with 10% Fetal Bovine Serum (Gemini) plated in the outer chamber. After 48 hours at 37° C, Transwell plates were fixed in 4% formaldehyde, stained with 0.5% crystal violet, and washed in DI water. Stained plates were left to air dry at room temperature for 24 hours and placed on microscopy slides. Slides were photographed and analyzed using ImageJ (https://imagej.net/) software using the Threshold and Measure tools to match covered area visually.

Quantitative Real-Time PCR (qRT-PCR) analysis of RNA

RNA extractions and purifications were performed using Qiazol and RNeasy Kit (Qiagen). Reverse transcription was performed with MultiScribe™ Reverse Transcription kit (Invitrogen). RNA Expression was determined using Taqman quantitative real-time PCR

using 0.6% Platinum® Taq DNA Polymerase (Invitrogen), 2% ROX Reference Dye (Invitrogen), 0.2 mM of dNTPs (our lab), 0.6 μM of each primer, and 0.33 μM of probe per reaction on 25 ng/μL of DNA template with the following primer-probe sets: Forward Primer GGAAGCCCATGATCATCTACAA, Reverse Primer ACAAAGGCATCGTTGGAGT, and probe GCAATACCTCAACAGCCCGGGT were used for detection of *WT-GSN*. Forward Primer CTGAAACCTCCCAGCTCAAT, Reverse Primer ACAAAGGCATCGTTGGAGT, and probe GCAATACCCCGTCATTCACCAT were used for detection of endogenous *ASE-GSN*. Forward Primer CCTGTCCAGAGCCGTGT, Reverse Primer ATTGAGCTGGGAGGTTTCAG, and probe AGGACCTGGAAATTACCTCAACAGCCC were used for detection of the ectopic *ASE-GSN* plasmid. All assays were quantified in triplicate against a *GAPDH* control 20X Gene Expression Assay (Invitrogen) using the $2^{-\Delta\Delta CT}$ method. (24–26)

Western Blotting

Protein extraction was performed with 10% RIPA Lysis Buffer (Upstate) with Complete Mini (Roche) and PhosphStop (Roche) inhibitors. Proteins were developed in Pierce 660 nm Protein Assay (Thermo Scientific, 22660) and quantified by absorption at 660 nm Spectramax M2 against bovine serum albumin (Sigma-Aldrich) standard curve. SDS-PAGE was performed on Criterion XT Precast Gel (Bio-Rad) per manufacturer's instructions. Blotting performed with Gelsolin Rabbit mAb (D9W8Y, Cell Signaling Technology [CST]), and GAPDH XP® Rabbit mAb (D16H11, CST) primary antibodies. Secondary antibody Anti-rabbit IgG, HRP-linked Antibody (7074S, CST) was used with Amersham ECL Prime Western Blotting Detection Reagent (GE Healthcare). Notably, D9W8Y Gelsolin antibody bound to N-terminus of the protein and almost exclusively detected full-length *WT-GSN* due to its abundant expression relative to other *GSN* isoforms. Since the endogenous expression of all other *GSN* isoforms, including *ASE-GSN*, is much lower, they were not detected using Western Blotting. D9W8Y Gelsolin antibody detected ectopically expressed *ASE-GSN* in knock-in experiments. There is no other high-quality *GSN* antibody on the market. The Western Blotting images were quantified with ImageJ (https://imagej.net/) software, by creating density histograms and measuring the area under the curve with the magic wand tool. Antibody binding to GSN was calculated relative to GAPDH.

Statistical Analysis

Outlier Gene Set Analysis - OGSA—OGSA p-value was calculated using a Fisher exact test comparing the number of outliers occurring in tumors with normal as it was previously done in Guo et al (2)

Student t-test—Student t-test was used to compare cells with and without treatment for experiments performed in triplicates or pentaplicates. P-values below 0.05 were considered significant.

RESULTS:

High rate of *GSN* ASEs in primary HNSCC tumor samples

Our recent analysis of ASE distribution in HNSCC samples using RNA-Seq data revealed 109 ASE junctions with high specificity to tumor samples. (2) Among these tumorspecific splice variants, a recurring splice junction was identified within the *GSN* gene at a noncanonical chr9: 124089070−124089586 junction (**Fig. 1**). Of the 46 HNSCC samples, 18 (39%) were outliers with respect to normalized expression of the *GSN* alternative splice junctions and no outliers were found in the 25 normal control samples (OGSA p=0.0015, **Fig 1A**). The preferential expression of *ASE-GSN* in HNSCC tumor samples was previously reported for the TCGA (The Cancer Genome Atlas) cohort. (2, 15) In opposite, the average *WT-GSN* expression in tumor and normal samples was not significantly different by OGSA (**Fig 1B**).

Molecular structure effects of *GSN* alternative splicing

The full-length *WT-GSN* is composed of 17 exons expressed from Chromosome 9 (**Supplemental Fig 2**). (27) The non-canonical ASE junction between 124089070−124089586 bp results in a 110 bp insertion between exons 14 and 15, found primarily in tumor samples (**Fig 1C**). This cancer-specific insert codes for 33 extra amino acids and contains a TGA stop codon after first 99 bp (**Supplemental Fig 1**), which leads to the expression of a truncated *ASE-GSN* protein. The full-length *WT-GSN* protein, which consists of 6 gelsolin domains G1, G2, G3, G4, G5, and G6 that fold to form the active tertiary structure of the protein, was visualized with InterPro© analysis.(28–30) (**Fig 1D, bottom**) *WT-GSN* folds upon itself by a Ca^{2+} dependent latch between G2 and G6, which locks the protein in a closed, inactive conformation. (29, 31, 32) **(Fig 1D)** The tumor-specific ASE-mRNA encodes only for the G1, G2, G3, and G4 gelsolin domains (**Fig 1E, top**), while losing the G5 and G6 subunits, where the latter is critical for the Ca^{2+} latch (Fig 1D).

Total *GSN* expression affects cell proliferation and viability

To determine the translational value of acquired data to the clinical application, the functional effects of *GSN* alternative splicing on cellular function were verified by complimentary *in vitro* techniques, such as proliferation and invasion assays. First, expression of *ASE-GSN* in HNSCC cell lines was cross-validated in 19 Head and Neck Tumor cell lines and three oral keratinocyte cell lines. (**Supplemental Table 1**) We have not detected any statistical significance by OGSA in either *ASE-GSN* or *WT-GSN* expression (**Supplemental Fig 3**). From this panel of HNSCC cell lines, UM-SCC-22B and SCC61 cells were chosen for functional evaluation due to their high invasive potential.

Ectopic knock-in expression of both *WT-GSN* and *ASE-GSN* isoforms in UM-SCC-22B (t-test p_{WT}=0.05 and p_{ASE}=0.0001, **Supplemental Fig 4A and 4B, as well as 4C, 4D, and 4I**) and SCC61 (p_{WT}=0.02 and p_{ASE}=0.00001, **Supplemental Fig 4E and 4F, as well as 4G, 4H, and 4I**) decreased proliferation of UM-SCC-22B (Fig 2A) and SCC61 (Fig 2B) cells over time. Conversely, siRNA downregulation of both *WT-GSN* and *ASE-GSN* in UM-SCC-22B (p_{pool}=0.005, p_{si1}=0.0002, and p_{si2}=0.04, **Supplemental Fig 5A and 5B, as well**

as 5C and 5G) and SCC61 (p_{pool}=0.00001, p_{si1}=0.003, and p_{si2}=0.25, **Supplemental Fig 5D and 5E, as well as 5F and 5G**) increased cell proliferation over time in UM-SCC-22B (Fig 2C) and SCC61 (Fig 2D) cells. Notably, *ASE-GSN* siRNA2 did not work well for SCC61 (p=0.25, **Supplemental Fig 5E**) due to some undetected genomic or transcriptomic variability. *ASE-GSN* siRNA1 worked better for both UM-SCC-22B and SCC61 (**Supplemental Fig 5B and 5E**). These data suggest that overall levels of total *GSN* played a role in the regulation of cellular viability and proliferation related to carcinogenesis.

ASE-GSN expression modulates the metastatic potential of cancer cells

Ectopic knock-in expression of *ASE-GSN* in UM-SCC-22B (p=0.0001, **Supplemental Fig 4B, as well as 4I**) and SCC61 (p=0.00001, **Supplemental Fig 4F, as well as 4I**) increased cellular invasion of UM-SCC-22B (p=0.0881, Fig 3A) and SCC61 cells (p=0.0460, Fig 3B). In contrast, ectopic expression of *WT-GSN* in UM-SCC-22B (p=0.05, **Supplemental Fig 4A, as well as 4I**) and SCC61 (p=0.02, **Supplemental Fig 4E, as well as 4I**) decreased cellular invasion of UM-SCC-22B (p=0.0258, Fig 3C) and SCC61 (p=0.33, Fig 3D) HNSCC cell lines. Conversely, siRNA downregulation of *ASE-GSN* expression in UM-SCC-22B (p_{si1}=0.0002 and p_{si2}=0.04, **Supplemental Fig 5B**) and SCC61 (p_{si1}=0.003 and p_{si2}=0.25, **Supplemental Fig 5E**) decreased cellular invasion of UM-SCC-22B (p_{si1}= 0.0232 and p_{si2}= 0.0092, Fig 4A) and SCC61 (p_{si1}= 0.0289 and p_{si2}= 0.5209, Fig 4B) cells. Notably, low efficiency of *ASE-GSN* siRNA2 in SCC61 (p=0.25, **Supplemental Fig 5E**) can explain non-significant invasion changes (p=0.5, Figure 4B) in this cell line. Conditional siRNA downregulation of *WT-GSN* expression in UM-SCC-22B (p_{pool}=0.005, **Supplemental Fig 5A, as well as 5C and 5G**) and SCC61 (p_{pool}=0.00001, **Supplemental Fig 5D, as well as 5F and 5G**), which was confirmed with strong concordance between RNA- and protein-based detection, increased cellular invasion of UMSCC-22B (p_{pool}= 0.0016, Fig 4C) and SCC61 (p_{pool}= 0.0021, **Fig 4D)**. This data suggests that the effects of *GSN* on invasion may be isoform specific. Given the ability of *GSN* to sever actin filaments, it is possible that *ASE-GSN* may increase tumor invasion and metastatic potential.

DISCUSSION:

Prior literature has shown that *GSN* has multifunctional roles in actin remodeling, PI3K/mTOR/AKT signaling, and apoptosis. (16, 29, 31–33) Given the significance of these cellular functions to metastatic potential, and considering the 109 ASE-genes we previously found in HNSCC (2), we focused on the functional analysis of *ASE-GSN*. Prior research suggested a paradoxical role for *GSN*, in some instances increasing apoptosis and in others increasing metastasis. (34–38) The results of our study provide new evidence that may help clarify the influence of *GSN* on cellular survival, at least with respect to HNSCC. In this discussion, we propose a model that is consistent with our data and with prior research, which illustrates possible roles for both *ASE-GSN* and *WT-GSN* in metastatic and apoptotic processes.

Until now, the role of non-canonical *GSN* alternative splicing in tumor samples has remained uncharacterized. Literature does suggest the expression of other canonical *GSN* splice sites that result in translation of 19 isoforms of *GSN*, (27) but their correlation with

disease status was not evaluated in our paper because they were not detected in our initial discovery cohort. The existence of differential expression of *GSN* suggests that *GSN* isoforms may play a role in regulating oncogenic behaviors, such as apoptosis and proliferation. The overall expression of both *ASE-GSN* and full-length *WT-GSN* isoforms have an inverse relationship with cell viability and proliferation (Fig 2), which is consistent with available literature that documents the role of *GSN* in apoptotic pathways. (31) *GSN* can either increase or decrease apoptosis, depending on the cellular conditions and the specific tissue or cell type in which it is expressed (Fig 5). Caspase-3 cleaves *GSN* between the 352nd and 353rd residues, resulting in C-*GSN* and N-*GSN* (with three gelsolin subunits each). N-*GSN* protein can cleave actin-independent of Ca^{2+}, which induces apoptotic morphological changes within the cell. (17)

Full-length *GSN* binds to actin non-competitively with DNase I, but N-*GSN* binds competitively, resulting in the increased cellular valence of DNase I, leading to enhanced apoptotic activity. (31) In our study, ectopic knock-in expression of either *WT-GSN* or *ASE-GSN* led to reduced cell proliferation over time. This observation suggests that the overall level of total *GSN* (WT or ASE) influences cell survival. One possibility, consistent with these observations, is that the overexpression of cellular *GSN* (ASE or WT) levels results in higher rates of cleavage of *GSN* to N-*GSN*, resulting in higher downstream levels of active DNase I, inducing Ca-independent apoptosis (Fig 5 *middle*). Invasion of cells through the basement membrane, an important hallmark of cancer cells, was increased with higher expression of *ASEGSN* (**Fig 3A and 3B**) and decreased with reduced expression of *ASE-GSN* (**Fig 4A and 4B**). Furthermore, increased expression of *WT-GSN* lowered invasion (**Fig 3C and 3D**) of cells and decreased expression of *WT-GSN* promotes invasion (**Fig 4C and 4D**). Given the important role of *GSN* as actin-regulating protein, any slight changes in localization or activity of GSN would significantly affect cell migration and metastatic potential. Indeed, current literature supports our observations; it has been seen that the Ca^{2+} dependency of *GSN* is largely dependent on the C-terminus and that the metastatic suppressor qualities of *GSN* are determined by the presence of this C-terminus. (32) The tertiary structure of *GSN* proposed by (28) and (31) contains a “latch” between the G2 and G6 subunits that is dependent upon Ca^{2+} for release and activation of *GSN* actin binding (**Fig 5 top**). The G1, G2, and G3 subunits necessary for actin severing are still preserved in *ASE-GSN*. (16, 30, 31)

We propose a model in which *ASE-GSN* does not contain this latch and is thus able to bind to actin in a Ca^{2+} independent manner (**Fig 5 bottom**) while maintaining non-competitive binding with DNase I, unbalancing pathways critical in normal cell physiology. (17, 29) The difference in ability to unlatch could result in equal effects of *ASE-GSN* and *WT-GSN* upon cell proliferation and survival, but cause increased actin severing and metastasis when there is a high ASE/WT *GSN* ratio (Fig 5).

Although various sources have described the mechanism by which *GSN* binds actin, *GSN* has a seemingly paradoxical relationship with the PI3K/AKT/mTOR pathway. *GSN* has been previously shown to dysregulate the PI3K/AKT/mTOR pathway, bind actin monomers in a Ca^{2+}-dependent manner, and cause severing of actin fibers. (16, 29, 32) A study by *Ma et al.* demonstrated that *GSN* upregulated pAKT, promoting survival in osteosarcoma, but

another study by *Yeh et al.* demonstrated that *GSN* downregulated pAKT, causing death in hypoxic cardiomyoblast cells. (39, 40) Our data establish that alternative splicing of the *GSN* gene has potential to resolve this apparent contradiction.

In surgically resected non-small cell lung cancer, a loss of *GSN* expression has been observed by IHC. (34) In contrast, *GSN* expression in cervical carcinoma has been reported to be upregulated relative to the surrounding tissue. (35) Similarly, *GSN* expression in hepatocellular carcinoma has been found to be overexpressed relative to adjacent tissue. (36) An *in vitro* study by Zhuo et al. found that expression of *GSN* in colorectal cancer cells was necessary for invasion through matrigel. (37) However, overexpression of *GSN* in the NK lymphoma cell line YTS has been reported to increase apoptosis and decrease cell proliferation and invasion. (38)

Considering the inconsistencies in the prior literature, our observations support a model in which *ASE-GSN* promotes invasion, whereas *WT-GSN* promotes either apoptosis or invasion, dependent on overall levels of *GSN expression*. However, from our observations in this study, we cannot be certain that *ASE-GSN* promotes metastasis *in vivo*. Alternative explanations are possible for the upregulation of *ASE-GSN* that we observed in HNSCC. For example, the existence of *ASE-GSN* might be in some way related to alterations in tensile stress acting upon cell membranes within the tumor microenvironment (41). Future research could explore, through an *in vivo* xenograft model, whether *ASE-GSN* indeed promotes metastasis.

Additional study is also needed to elucidate the link between *GSN* isoforms and AK-Tregulated apoptosis, migration, and proliferation. Our proposed model requires further investigation into the effects of Ca^{2+} on isoform-specific actin-severing activity. Future studies of *GSN* should include analysis of the effects of calcium availability on downstream isoform-specific regulation. Further investigation is necessary to elucidate whether *GSN* effects on the PI3K/AKT/mTOR pathway are playing a role in *GSN*-mediated cell death. Prospectively, it would be interesting to identify different isoforms of *GSN,* using modern long-range RNA-Seq and computational technologies, such as CLASS2 (42, 43) or SUPPA (44). Their role in clinical outcome can be further evaluated in a larger clinical cohort.

Validation of alternative splicing in oncogenesis could improve both diagnosis and treatment of HNSCC. Over the past 30 years, there has been limited change in the treatment protocol for HNSCC. A better understanding of alternative splicing in cancer may open new avenues for future disease treatment such as generating new cancer-specific immunotherapeutics targeted against alternatively spliced proteins, neoantigens for immunotherapeutics, or biomarkers for detection and prognostication of disease. Specifically, if *ASE-GSN* protein were shown to be carcinogenic, monoclonal antibody drugs could be developed to target the unique epitope of *ASE-GSN* isoform. Due to the unique sequence of *ASE-GSN* predominately expressed in the tumor (outlier detection rates 39%), but not in normal samples (specificity 100%), this *ASE-GSN* junction may be used for detection purposes. Moreover, *ASE-GSN* or other cancer-specific ASEs can be detected by IHC analysis of pathology samples during cancer diagnostics. Currently, Human papillomavirus (HPV) *in situ* hybridization and immunostaining of surrogate HPV+ marker protein p16 are the only

clinical marker of HNSCC. (45) Our data suggest that, because ASE outliers are found in 39% of cases, ASE might have 39% sensitivity with ultimate near 100% specificity for detection of cancerous tissues. This observation suggests that ASEs could help bolster specificity during HNSCC testing. Furthermore, using this method of detection would identify specific subsets of cancers with distinct biology, which may facilitate specifically targeted treatment regimens. This work will build a basis for the development of ASE-specific cancer biomarkers, which can potentially be used for primary and secondary detection and cancer surveillance using biopsy and biofluids, directly characterizing tumors without reliance on surrogate protein techniques.

Supplementary Material

Refer to Web version on PubMed Central for supplementary material.

ACKNOWLEDGMENTS

All authors have read the journal's authorship agreement and the journal's policy on disclosure of potential conflicts of interest. EJW is CEO of Maryland Holistics LLC, all other authors declared no conflict of interest.

This work was supported by NIH grants R21DE025398 (DAG), 5P50DE019032 (DAG and EJF), P30CA006973(EJF, LVD, and AVF).

Financial support: Daria A. Gaykalova – R21DE025398

REFERENCES

1. Banister CE, Liu C, Pirisi L, Creek KE, Buckhaults PJ. Identification and characterization of HPV-independent cervical cancers. Oncotarget. 2017;8(8):13375–86. [PubMed: 28077784]
2. Guo T, Sakai A, Afsari B, Considine M, Danilova L, Favorov AV, et al. A Novel Functional Splice Variant of AKT3 Defined by Analysis of Alternative Splice Expression in HPV-Positive Oropharyngeal Cancers. Cancer Res 2017;77(19):5248–58. [PubMed: 28733453]
3. Rea Li. Expression microarray analysis reveals alternative splicing of LAMA3 and DST genes in head and neck squamous cell carcinoma. PLoS One. 2014;9:e91263. [PubMed: 24675808]
4. Körner M, Miller LJ. Alternative Splicing of Pre-mRNA in Cancer: focus on G protein-coupled peptide hormone receptors. The American journal of pathology. 2009;175(2):461–72. [PubMed: 19574427]
5. The Cancer Genome Atlas Network. Comprehensive genomic characterization of head and neck squamous cell carcinomas. Nature. 2015;517:576–82. [PubMed: 25631445]
6. Boscolo-Rizzo P, Del Mistro A, Bussu F, Lupato V, Baboci L, Almadori G, et al. New insights into human papillomavirus-associated head and neck squamous cell carcinoma. Acta Otorhinolaryngol Ital 2013;33(2):77–87. [PubMed: 23853396]
7. Suresh T, Burtness B. The Emerging Role of Immunotherapy in Head and Neck Squamous Cell Cancer. AJHO. 2017;13(6):20–7.
8. Cognetti DM, Weber RS, Lai SY. Head and neck cancer: an evolving treatment paradigm. Cancer. 2008;113(7 Suppl):1911–32. [PubMed: 18433484]
9. US Food & Drug Administration. pembrolizumab (KEYTRUDA) Silver Spring, MD: US Food & Drug Administration; 2016 [updated 08/09/2016 Available from: https://www.fda.gov/Drugs/InformationOnDrugs/ApprovedDrugs/ucm515627.htm.
10. US Food & Drug Administration. Nivolumab for SCCHN Silver Spring, MD: US Food &Drug Administration; 2016 [updated 11/10/2016 Available from: https://www.fda.gov/Drugs/InformationOnDrugs/ApprovedDrugs/ucm528920.htm.
11. Ran X, Yang K. Inhibitors of the PD-1/PD-L1 axis for the treatment of head and neck cancer: current status and future perspectives. Drug design, development and therapy. 2017;11:2007–14.

12. Mea Ochs. Outlier Analysis and Top Scoring Pair for Integrated Data Analysis and Biomarker Discovery. IEEE/ACM Trans Comput Biol Bioinform. 2013:[Epub ahead of print].
13. Jea MacDonald. COPA--cancer outlier profile analysis. Bioinformatics.2006;22(23):2950–1. [PubMed: 16895932]
14. Guo T, Gaykalova DA, Considine M, Wheelan S, Pallavajjala A, Bishop JA, et al. Characterization of functionally active gene fusions in human papillomavirus related oropharyngeal squamous cell carcinoma. Int J Cancer. 2016;139(2):373–82. [PubMed: 26949921]
15. Sebestyen E, Zawisza M, Eyras E. Detection of recurrent alternative splicing switches in tumor samples reveals novel signatures of cancer. Nucleic Acids Res 2015;43(3):1345–56. [PubMed: 25578962]
16. Fujita H, Laham LE, Janmey PA, Kwiatkowski DJ, Stossel TP, Banno Y, et al. Functions of [His321]gelsolin isolated from a flat revertant of ras-transformed cells. Eur J Biochem 1995;229(3):615–20. [PubMed: 7758454]
17. Kothakota S, Azuma T, Reinhard C, Klippel A, Tang J, Chu K, et al. Caspase-3generated fragment of gelsolin: effector of morphological change in apoptosis. Science (New York, NY). 1997;278(5336):294–8.
18. Hanahan D, Weinberg RA. Hallmarks of Cancer: The Next Generation. Cell. 2011;144(5):646–74. [PubMed: 21376230]
19. Winston JS, Asch HL, Zhang PJ, Edge SB, Hyland A, Asch BB. Downregulation of gelsolin correlates with the progression to breast carcinoma. Breast Cancer Res Treat 2001;65(1):11–21. [PubMed: 11245335]
20. Hatakeyama H, Cheng H, Wirth P, Counsell A, Marcrom SR, Wood CB, et al. Regulation of heparin-binding EGF-like growth factor by miR-212 and acquired cetuximab-resistance in head and neck squamous cell carcinoma. PLoS One. 2010;5(9):e12702. [PubMed: 20856931]
21. Gaykalova D, Vatapalli R, Glazer CA, Bhan S, Shao C, Sidransky D, et al. Dosedependent activation of putative oncogene SBSN by BORIS. PLoS One. 2012;7(7):e40389. [PubMed: 22792300]
22. Ahmed SA, Gogal RM, Walsh JE. A new rapid and simple non-radioactive assay to monitor and determine the proliferation of lymphocytes: an alternative to [3H]thymidine incorporation assay. Journal of Immunological Methods. 1994;170(2):211–24. [PubMed: 8157999]
23. Magro A Apoptotic Events in Glioma Activate Metalloproteinases and Enhance Invasiveness, Fairmont, WV, USA2013 [updated Feb 27.
24. Livaka KJ, Schmittgen TD. Analysis of Relative Gene Expression Data Using Real-Time Quantitative PCR and the 2−ΔΔCT Method. Methods. 2001;25(4):402–8. [PubMed: 11846609]
25. Pierce D Real-Time PCR: the TaqMan Method Davidson, NC, USA2003 [cited Davidson College.
26. Gaykalova DA, Zizkova V, Guo T, Tiscareno I, Wei Y, Vatapalli R, et al. Integrative computational analysis of transcriptional and epigenetic alterations implicates DTX1 as a putative tumor suppressor gene in HNSCC. Oncotarget. 2017;8(9):15349–63. [PubMed: 28146432]
27. Kent WJ, Sugnet CW, Furey TS, Roskin KM, Pringle TH, Zahler AM, et al. The human genome browser at UCSC. Genome Res 2002;12(6):996–1006. [PubMed: 12045153]
28. Cea Lv. Single-molecule force spectroscopy reveals force-enhanced binding of calcium ions by gelsolin. Nat Commun 2014;5:4623. [PubMed: 25100107]
29. dos Remedios CG, Chhabra D, Kekic M, Dedova IV, Tsubakihara M, Berry DA, et al. Actin binding proteins: regulation of cytoskeletal microfilaments. Physiol Rev 2003;83(2):433–73. [PubMed: 12663865]
30. Jones P, Binns D, Chang HY, Fraser M, Li W, McAnulla C, et al. InterProScan 5: genome-scale protein function classification. Bioinformatics. 2014;30(9):1236–40. [PubMed: 24451626]
31. Li GHea. Multifunctional Roles of Gelsolin in Health and Disease. Medicinal Research Reviews. 2010;32(5):999–1025. [PubMed: 22886630]
32. Fujita H, Okada F, Hamada J-i, Hosokawa M, Moriuchi T, Chikara Koya R, et al. Gelsolin Functions as a Metastasis Suppressor in B16-BL6 Mouse Melanoma Cells and Requirement of the Carboxyl-Terminus for its Effect. Int J Cancer. 2001;93(6):773–80. [PubMed: 11519036]

33. Molinolo AA, Amornphimoltham P, Squarize CH, Castilho RM, Patel V, Gutkind JS. Dysregulated molecular networks in head and neck carcinogenesis. Oral Oncol 2009;45(4– 5):324–34. [PubMed: 18805044]
34. Dosaka-Akita H, Hommura F, Fujita H, Kinoshita I, Nishi M, Morikawa T, et al. Frequent loss of gelsolin expression in non-small cell lung cancers of heavy smokers. Cancer Res 1998;58(2):322–7. [PubMed: 9443412]
35. Liao CJ, Wu TI, Huang YH, Chang TC, Wang CS, Tsai MM, et al. Overexpression of gelsolin in human cervical carcinoma and its clinicopathological significance. Gynecol Oncol 2011;120(1):135–44. [PubMed: 21035170]
36. Deng B, Fang J, Zhang X, Qu L, Cao Z, Wang B. Role of gelsolin in cell proliferation and invasion of human hepatocellular carcinoma cells. Gene. 2015;571(2):292–7. [PubMed: 26149653]
37. Zhuo J, Tan EH, Yan B, Tochhawng L, Jayapal M, Koh S, et al. Gelsolin induces colorectal tumor cell invasion via modulation of the urokinase-type plasminogen activator cascade. PLoS One. 2012;7(8):e43594. [PubMed: 22927998]
38. Guo Y, Zhang H, Xing X, Wang L, Zhang J, Yan L, et al. Gelsolin regulates proliferation, apoptosis and invasion in natural killer/T-cell lymphoma cells. Biol Open 2018;7(1).
39. Ma X, Sun W, Shen J, Hua Y, Yin F, Sun M, et al. Gelsolin promotes cell growth and invasion through the upregulation of p-AKT and p-P38 pathway in osteosarcoma. Tumour Biol 2016;37(6):7165–74. [PubMed: 26662962]
40. Yeh Y-L, Ting W-J, Shen C-Y, Hsu H-H, Chung L-C, Tu C-C, et al. Hypoxia Augments Increased HIF-1α and Reduced Survival Protein p-Akt in Gelsolin (GSN)-Dependent Cardiomyoblast Cell Apoptosis. Cell Biochem Biophys 2016;74(2):221–8. [PubMed: 27193608]
41. Bordeleau F, Califano JP, Negron Abril YL, Mason BN, LaValley DJ, Shin SJ, et al. Tissue stiffness regulates serine/arginine-rich protein-mediated splicing of the extra domain Bfibronectin isoform in tumors. Proc Natl Acad Sci U S A. 2015;112(27):8314–9. [PubMed: 26106154]
42. Song L, Florea L. CLASS: constrained transcript assembly of RNA-seq reads. BMC Bioinformatics. 2013;14 Suppl 5:S14.
43. Song L, Sabunciyan S, Florea L. CLASS2: accurate and efficient splice variant annotation from RNA-seq reads. Nucleic Acids Res 2016;44(10):e98. [PubMed: 26975657]
44. Alamancos GP, Pages A, Trincado JL, Bellora N, Eyras E. Leveraging transcript quantification for fast computation of alternative splicing profiles. RNA. 2015;21(9):1521–31. [PubMed: 26179515]
45. Singhi AD, Califano J, Westra WH. High-risk human papillomavirus in nasopharyngeal carcinoma. Head Neck. 2012;34(2):213–8. [PubMed: 21484924]

TRANSLATIONAL SIGNIFICANCE

We have recently detected the landscape of alternative splicing events in head and neck squamous cell carcinoma. In this work, we prove the oncogenic relevance of alternative splicing in Gelsolin through detailed functional validation. This data has direct clinical applications, where *ASE-GSN* can be used as a biomarker and a therapeutic target for HNSCC.

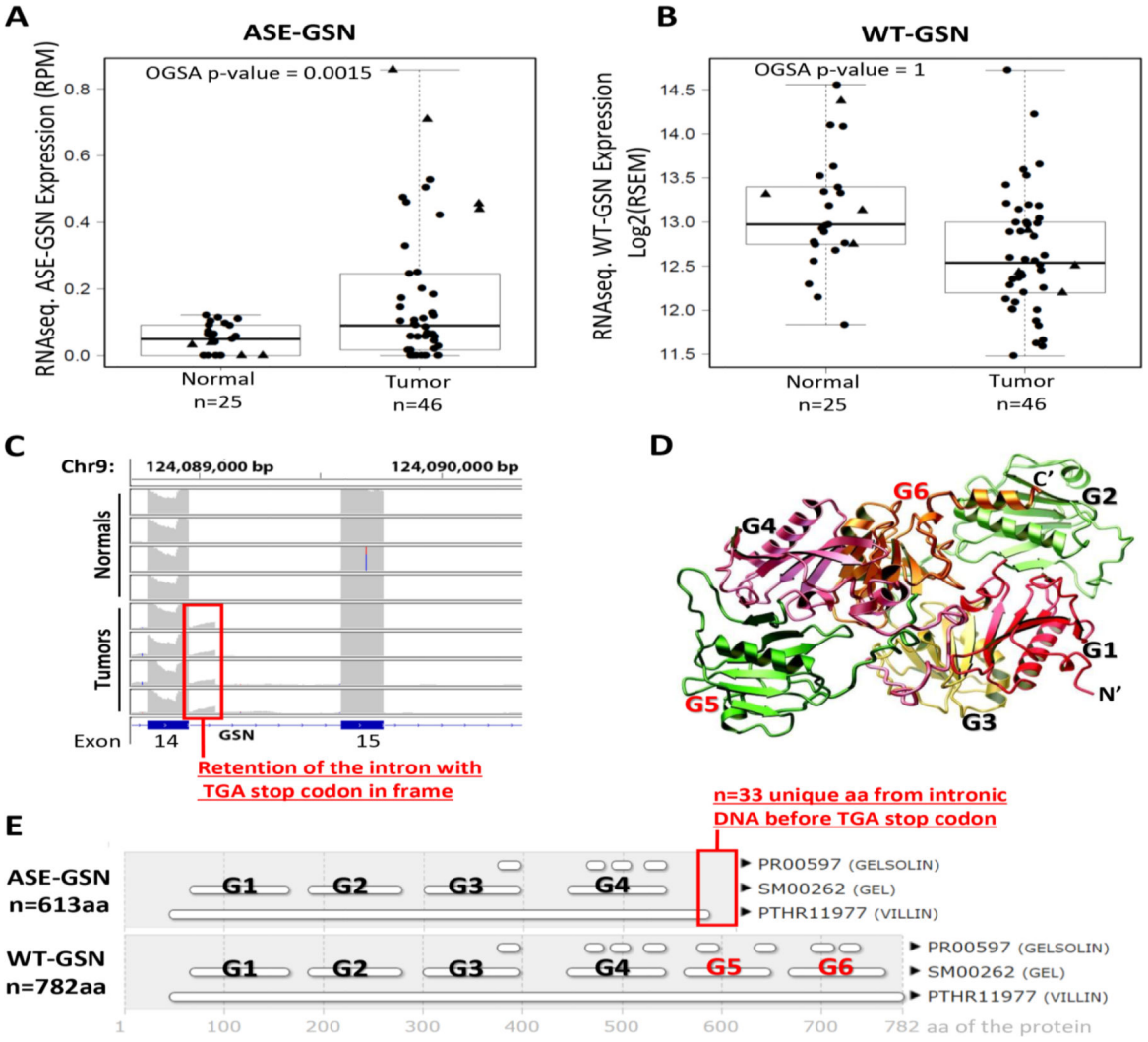

Figure 1. Discovery of *ASE-GSN* Expression in HNSCC samples.

(**A**) The box plot of the RPM expression of the alternative *GSN* junction (chr9:124089070 − 124089586) within the discovery cohort of 25 normal samples and 46 HNSCC samples. (2) The samples further illustrated in panel C are identified by triangle shape. Out of the 46 discovery cohort HNSCC samples, 18 outliers were discovered among normalized *GSN* junction expression in tumors, and no outliers were found in normal samples determined by OSGA, indicating significant outlier expression in cancerous phenotype (p=0.0015). (**B**) The boxplot of the logarithmic expression of the total *GSN* RSEM gene shows that total *GSN* expression is tumor and normals are not significantly different (OGSA p-value=1). The samples further illustrated in panel C are identified by triangle shape. (**C**) Integrative Genomic Viewer (IGV) visualization shows the alternative splicing event found between RefSeq Exon 14 and 15 of the *GSN* transcript, which produced the extended Exon 14 (red frame) expression in primary tumor samples, but not in normal controls. Notably, the tumor-specific extended Exon 14 has *TGA* stop codon in the frame, which causes the production of the truncated *ASE-GSN* protein. (**D**) The 3D crystal structure of *GSN* (29) with six GEL (G) domains, with G5 and G6 to be lost (red) due to the expression of the truncated *ASE-GSN*.

(**E**) The InterPro© analysis of the *ASE-GSN* (top, n=613 aa, including n=33 unique aa coded from the intronic DNA, red frame) and *WT-GSN* (bottom, n=782 aa) peptides revealed that the *WT-GSN* protein contains two extra GEL domains (red) not expressed in the truncated *ASE-GSN* protein.

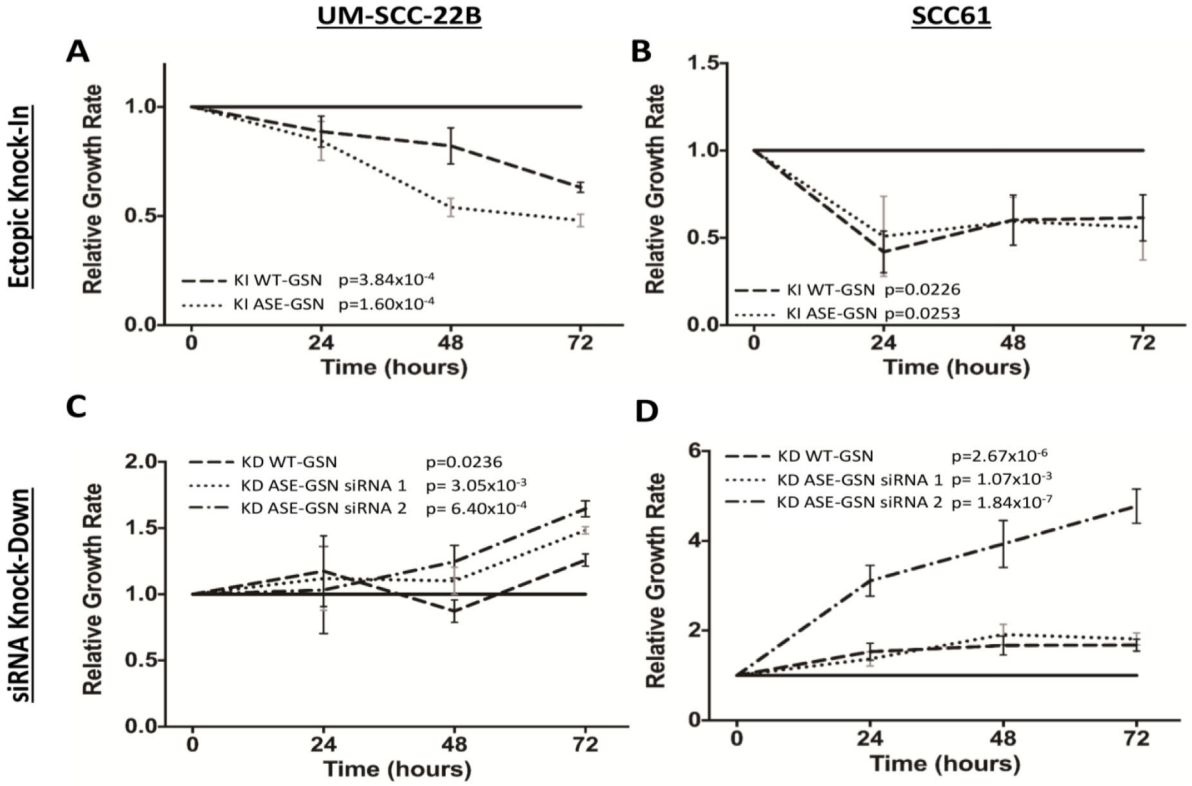

Figure 2. Cell proliferation in the presence and absence of *ASE-GSN* or *WT-GSN* expression.

The ectopic knock-in of *ASE-GSN* (dotted line) and *WT-GSN* (dashed line) isoform significantly decreased proliferation of UM-SCC-22B (**A**) and SCC61 (**B**) cells. The siRNA-mediated decrease of *ASE-GSN* (dotted line and dash-dot line) and *WT-GSN* (dashed line) isoforms significantly increased the proliferation of UM-SCC-22B (**C**) and SCC61 (**D**) cells. Error bars indicate normalized standard error calculated for each experiment. Significance determined by t-test comparison of 72-hour time-points normalize to starting emission between samples and controls.

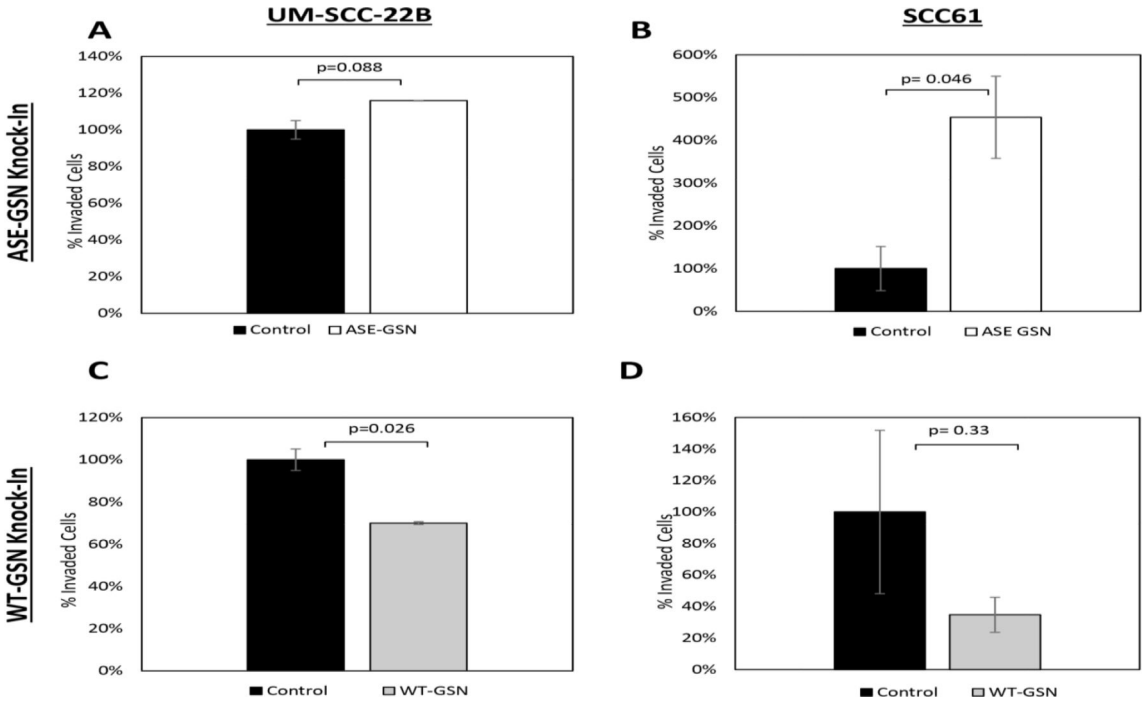

Figure 3. Cell migration and invasion in the presence of *ASE-GSN* or *WT-GSN* expression.

The ectopic expression of *ASE-GSN* (white) increased the cellular invasion and migration of UM-SCC-22B (**A**, p=0.088) and SCC61 (**B**, p=0.046) cells. The ectopic expression of *WT-GSN* (gray) decreased cellular invasion and migration of UM-SCC-22B (**C**, p=0.026) and SCC61 (**D**, p=0.33) cells. Asterisks indicate $p<0.05$. Error bars indicate normalized standard error calculated for each experiment.

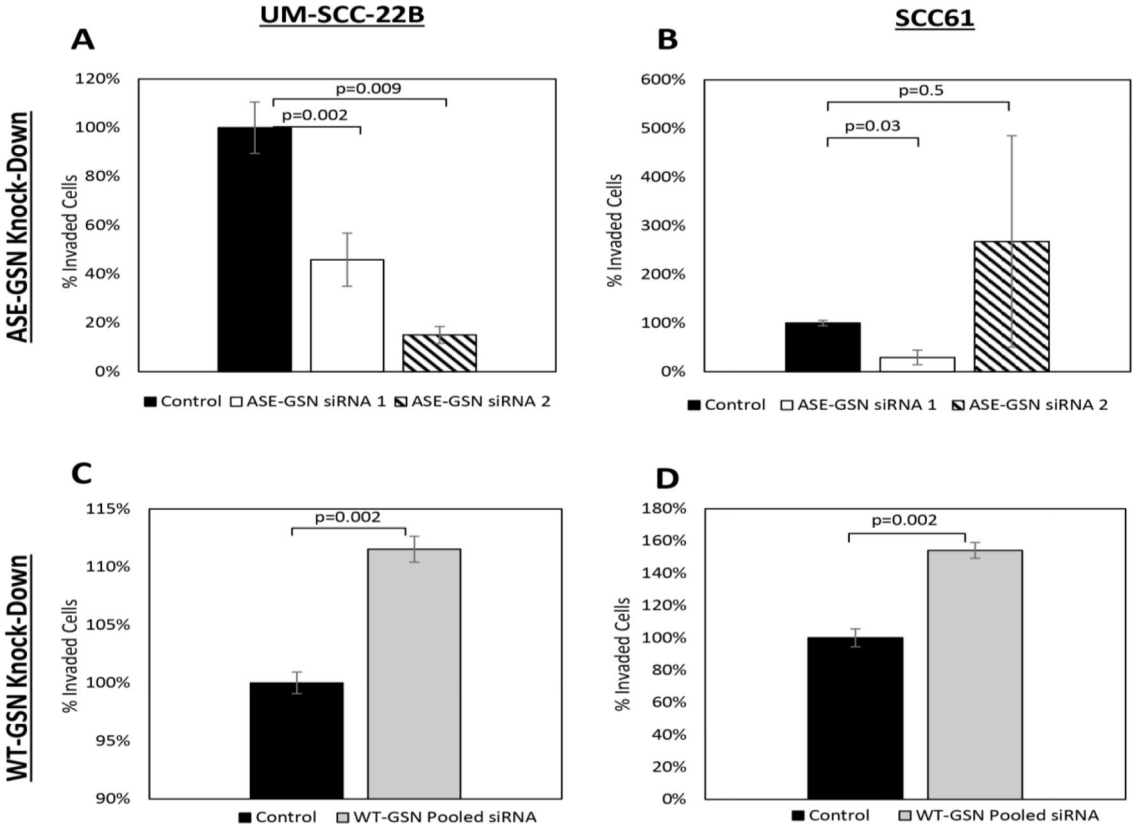

Figure 4. Cell migration and invasion in the absence of *ASE-GSN* or *WT-GSN* expression.

The siRNA-mediated decrease of *ASE-GSN* expression (white and striped bars) decreased the cellular invasion and migration of UM-SCC-22B (**A**, p=0.002, and p=0.009) and SCC61 (**B**, p=0.03, and p=0.5) cells. The siRNA-mediated decrease in *WT-GSN* expression significantly increased the cellular invasion and migration of UM-SCC-22B (**C**, p=0.0016) and SCC61 (**D**, p=0.002) cells.

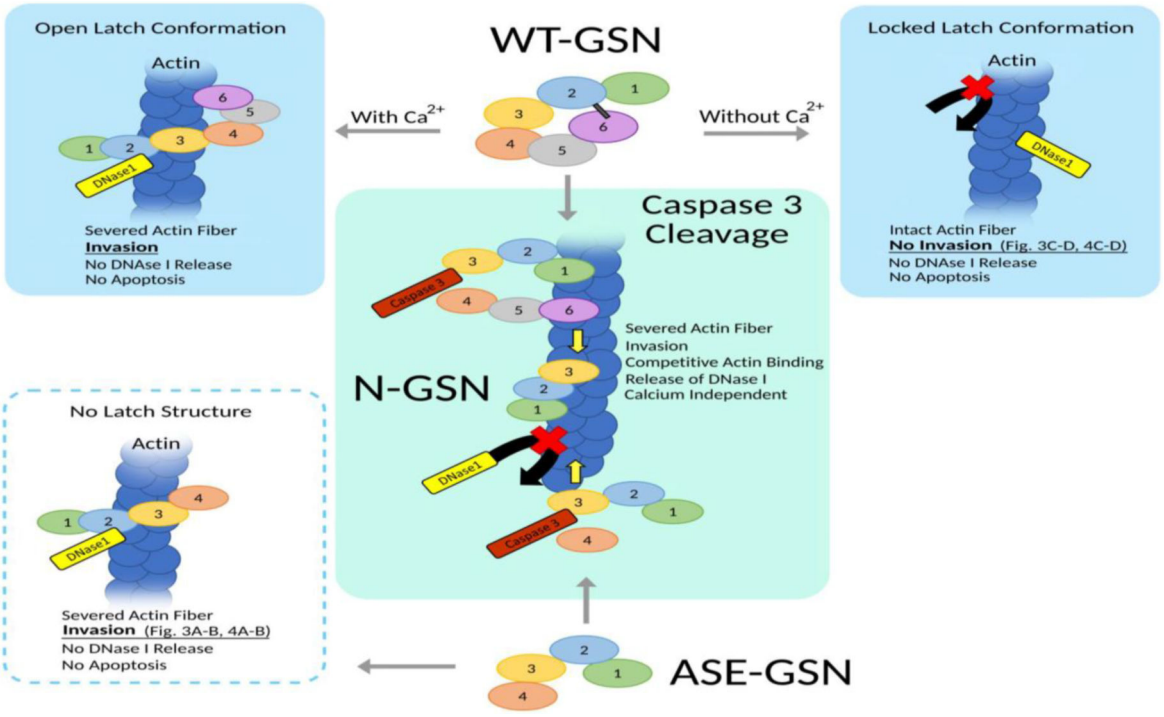

Figure 5. The proposed mechanism for the role of *GSN* isoform expression in apoptosis and metastasis.

Top Left: The full-length *WT-GSN* isoform contains a Ca^{2+} latch, which permits binding of *WT-GSN* to actin fiber only in the presence of Ca^{2+}. Binding of *WT-GSN* is noncompetitive with DNase I enzyme and does not induce apoptosis, but allows for GSN-mediated actin severing necessary for invasion. Top Right: In the absence of Ca^{2+} the full-length *WT-GSN* isoform is unable to bind actin. DNase I remains bound to actin and thus apoptosis is not induced. Actin is not severed, and thus invasion is not induced (relative to data shown in Figures 3C, 3D, 4C, and 4D). Bottom Left: The *ASE-GSN* isoform does not have a Ca^{2+} latch due to its truncated structure. Therefore, it can bind actin-independent of Ca^{2+} ions. As with *WTGSN*, binding of *ASE-GSN* is non-competitive with DNase I. Thus, DNase I remains bound to actin and apoptosis is not induced. In this model, binding of *ASE-GSN* causes actin severing, allowing for cell invasion (relative to data shown in Figures 3A, 3B, 4A, and 4B). Middle: Both *WT-GSN* and *ASE-GSN* are cleaved by Caspase-3, resulting in an N-*GSN* (subunits 1–3) fragment and a C-*GSN* (subunits 4–6) fragment. N-*GSN* binds actin in a Ca^{2+} independent manner competitive with DNase I, resulting in faster cleavage of the actin cytoskeleton and increased DNA degradation, stimulating apoptosis (relative to data shown in Figure 2). Furthermore, C-*GSN* is associated with invasion prevention, but C-*GSN* is only present in *WT-GSN* cleavage. Thus, *WT-GSN* offers protection from invasion, not provided by *ASE-GSN* (relative to data shown in Figures 3 and 4). (16, 17, 28, 29, 31, 32)